# Parameter dependence of homoclinic solutions in a single long Josephson junction

J.B. van den Berg, S.A. van Gils, T.P.P. Visser

October 4, 2001

**Abstract**

For a model of the long Josephson junction one can calculate for which parameter values there exists a homoclinic solution (fluxon solution). These parameter values appear to lie on a spiral. We show that this is a consequence of the presence of a heteroclinic solution, which lies at the centre of the spiral.

## 1 Introduction

A long Josephson junction is sketched in Figure 1. It consists of two slabs of superconducting material which have a small overlap and are separated by a thin insulating barrier. An important application of long Josephson junctions is their use as sub-millimeter radiation sources/detectors. To use such a junction as a radiation source, it has to be brought in a state where so-called fluxons travel along the junction. These fluxons are circulating currents which can release (some of) their energy in the form of radiation on collision with the edges of the device.

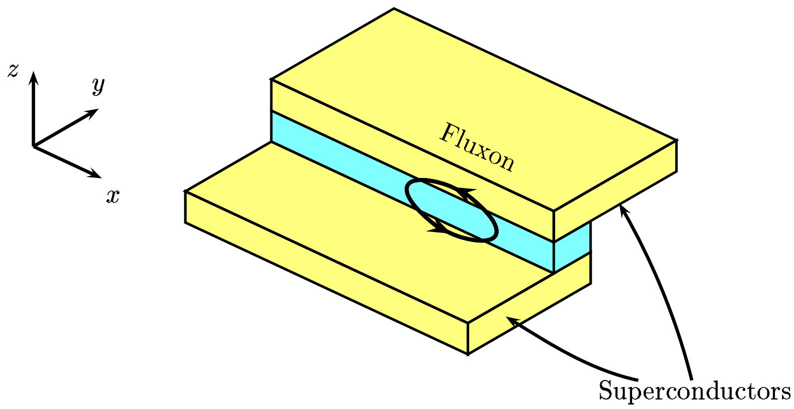


Figure 1: A sketch of a long Josephson junction

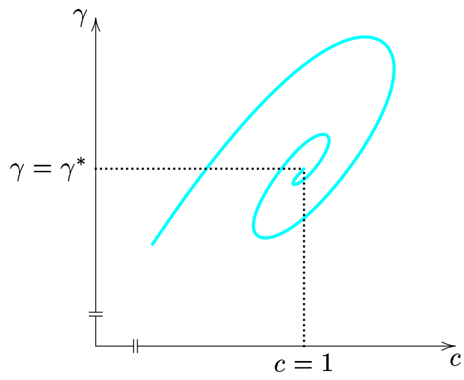


Figure 2: A sketch of the spiral in the $(c, \gamma)$-plane.

A model for the long Josephson junction is given by [1]

$$\Phi_{xx} - \Phi_{tt} - \sin\Phi = \alpha\Phi_t - \beta\Phi_{xxt} - \gamma. \tag{1}$$

In this equation $\Phi$ is the phase difference between the two superconducting layers and $x$ is the coordinate along the junction. The parameters $\alpha$ and $\beta$ are damping parameters (due to quasi-particles) and $\gamma$ is the bias current.

We look for travelling wave solutions of this equation and substitute $\Phi(x,t) = \phi(x+ct) = \phi(\xi)$ to get the equation

$$\beta c\phi''' + (1-c^2)\phi'' - \alpha c\phi' - \sin\phi + \gamma = 0. \tag{2}$$

This equation admits homoclinic solutions for certain combinations of $c$ and $\gamma$ (and fixed $\alpha$,$\beta$).

**1 Remark** *The variable $\phi$ is an angle-variable, so increasing its value by $2\pi$ has no effect on the system at all, hence a solution connecting the equilibria* $\arcsin\gamma$ *and* $\arcsin\gamma + 2\pi$ *is actually a* homoclinic *orbit.*

When calculating the parameter combinations for which a homoclinic orbit exists numerically (see e.g. [2]), one finds that they form a spiral in the $(c, \gamma)$-plane (Figure 2). The objective of this paper is to understand why this is a spiral. We shall show that this is a consequence of the fact that for certain parameter values, namely at the centre of the spiral, there exists a heteroclinic cycle. The centre of the spiral lies at a point $(c, \gamma) = (1, \gamma^*(\alpha, \beta))$; the significance of the special wave speed $c = 1$ is that Equation (2) has (additional) symmetries in that case (see section 2). When the parameters are varied one of the heteroclinic orbits breaks up and can form a homoclinic orbit.Such scenarios have been studied in a more general setting by Bykov [3]. We will prove the existence of the heteroclinic cycle at the centre of the spiral and give a simple version of the proof that this gives rise to homoclinic orbits for parameter values on a spiral.

To fix ideas let us now give an overview of the situation in phase space.

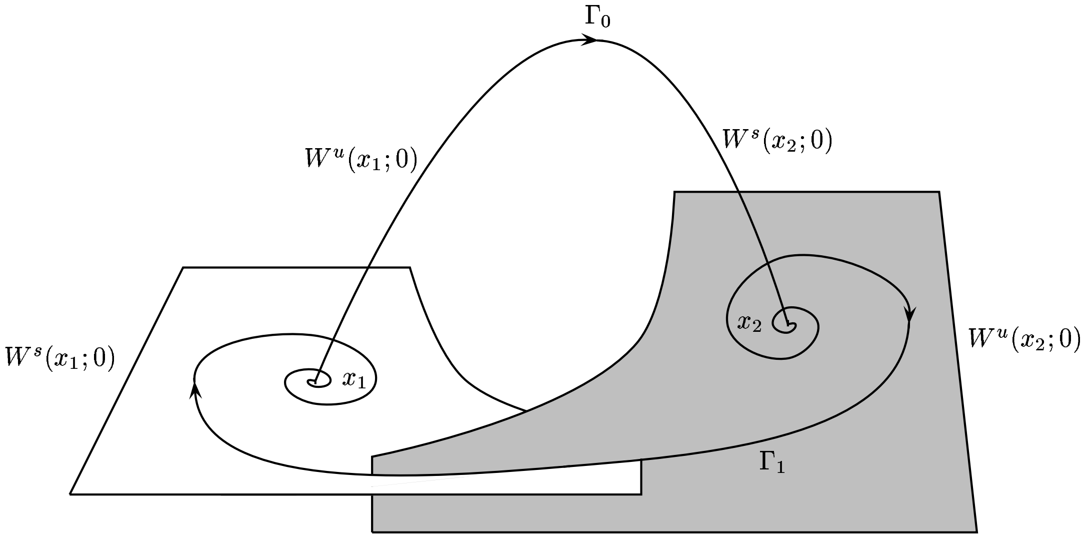


Figure 3: Heteroclinic cycle for $p = 0$

## 1.1 Sketch of the situation

Equation (2) has two equilibria (we identify the $2\pi$ shifted equilibria). We will fix the parameters $\alpha$ and $\beta$ since these are material properties and hence have two free parameters $c$ and $\gamma$.

The general picture is that we have an ordinary differential equation in $\mathbb{R}^3$ with a parameter $p \in \mathbb{R}^2$. For a special choice of $p$ the situation is as depicted in Figure 3: there is a heteroclinic cycle between the two equilibria. The one dimensional unstable manifold of equilibrium $x_1$ intersects the one dimensional stable manifold of $x_2$; this part of the heteroclinic cycle is non-generic (co-dimension 2). Furthermore, the two dimensional manifolds $W^u(x_2)$ and $W^s(x_1)$ intersect (transversally).

For parameter values different from this special choice, the unstable manifold of $x_1$ will no longer intersect the stable manifold of $x_2$. For specific choices of parameters, the unstable manifold may come close to the intersection of the two dimensional manifolds and intersect the stable manifold of $x_1$.

## 1.2 Outline

In section 2 we will prove the existence of the crucial heteroclinic connection. This is the main result. We will indicate the necessary conditions for the spiral to occur in section 3. In the following section we give the proof that these assumptions result in the spiral mentioned above. This is essentially the same as Lemma 4.1 in [3], but there the proof was part of a more general analysis and since we only need this specific item, the proof can be given in a more compact form. In the last section we show how the hypothesis needed for the proof can by verified numerically for the travelling waves in a long Josephson junction described by (1).

## 2 Existence of the heteroclinic connection

For $c = 1$ Equation (2) reduces (after rescaling) to

$$\phi''' - \tilde{\alpha}\phi' = \sin\phi - \gamma, \tag{3}$$

where $\tilde{\alpha} = \frac{\alpha}{\sqrt[3]{\beta}}$. For the rest of this section we will drop the tilde. This type of equation has been studied in [7]. However, we cannot simply refer to this paper because our right hand side is not sign definite.

The equilibria of (3) are given by

$$\phi_{2k} = 2k\pi + \arcsin\gamma, \quad \phi_{2k+1} = \pi - \arcsin\gamma + 2k\pi \tag{4}$$

Equation (3) is reversible and if $\phi(\xi)$ is a solution then so is $3\pi - \phi(-\xi)$. We will use these symmetries to prove the following result:

**2 Theorem** *There exists a constant $\alpha_0$ such that for all $0 < \alpha \leq \alpha_0$ there exists, for some $\gamma \in (0,1)$, a monotone symmetric (with respect to $\frac{3\pi}{2}$) heteroclinic solution connecting $\phi_0$ and $\phi_3$. Furthermore, $\alpha_0 > 0.65$.*

The linearised equation around $\phi_0$ has one positive eigenvalue $\lambda$, hence $\phi_0$ has a one dimensional unstable manifold for all $\gamma \in [-1, 1]$, which varies continuously with $\gamma$. We shoot, with $\gamma$ as the shooting parameter, from this (local) unstable manifold, where we take the orbit in $W^u_{\mathrm{loc}}$ which initially increases. Thus, for some small $\varepsilon > 0$ let $\phi(\xi, \gamma)$ be the solution of (3) with $\phi(0, \gamma) = \phi_0 + \varepsilon$ and $(\phi, \phi', \phi'')(0, \gamma) \in W^u_{\mathrm{loc}}(\phi_0, 0, 0)$.

Since we are looking for a monotone solution, it will be very helpful to use the following formulation. On intervals on which $\phi$ is monotonically increasing we define

$$t = \phi, \qquad z(t) = \frac{1}{2}\phi'(\xi)^2 \tag{5}$$

Then $\dot{z} = \phi''$, where the dot denotes differentiation with respect to $t$. For the second derivative of $z$ we find, using (3),

$$\ddot{z} = \alpha + \frac{\sin t - \gamma}{\sqrt{2z}}. \tag{6}$$

In the limit $\xi \to -\infty$, we find the initial value for the $z$-equation:

$$z(\phi_0) = 0, \quad \dot{z}(\phi_0) = 0, \quad \ddot{z}(\phi_0) = \lambda^2. \tag{7}$$

To set up the shooting method we define

$$\xi_1(\gamma) = \sup\{\tilde{\xi} \mid \phi''(\xi,\gamma) > 0 \text{ on } (-\infty,\tilde{\xi})\}, \tag{8}$$

$$\xi_2(\gamma) = \sup\{\tilde{\xi} \mid \phi(\xi,\gamma) < \frac{3\pi}{2} \text{ on } (-\infty,\tilde{\xi})\}. \tag{9}$$

Finally we define

$$\gamma_0 = \sup\{\gamma \in [-1,1] \mid \xi_1(\gamma) > \xi_2(\gamma)\}. \tag{10}$$

That $\gamma_0$ is well-defined follows from Lemma 3a below.

First we make some observations. Clearly $\phi'(\xi) > 0$ on $(-\infty, \xi_1]$. It follows from the implicit function theorem that $\xi_2(\gamma)$ depends continuously on $\gamma$ for $\gamma \le \gamma_0$. Besides, $\xi_2$ is finite for $\gamma \le \gamma_0$, since $\phi$ is concave on $(-\infty, \xi]$.

We shall prove the following properties.

**3 Lemma** *With the above definition of $\gamma_0$ one has*
*a. $\gamma_0$ is well-defined.*
*b. $\gamma_0 > 0$.*
*c. $\gamma_0 < 1$ for $0 < \alpha \le \alpha_0$, where $\alpha_0 \gtrapprox 0.65$.*

Before we prove this lemma, let us show how this leads to Theorem 2.

**4 Lemma** *For $\gamma = \gamma_0 \in (-1,1)$ one has $\xi_1 = \xi_2$.*

It follows that $\phi(\xi_1,\gamma_0) = \frac{3\pi}{2}$ and $\phi''(\xi_1,\gamma_0) = 0$, hence using the symmetry we have found for $\gamma = \gamma_0$ a heteroclinic solution as asserted in Theorem 2.

**Proof of Lemma 4:**
It follows from a continuity argument that $\xi_1(\gamma_0) \le \xi_2(\gamma_0)$. Now suppose, by contradiction, that $\xi_1 < \xi_2$ at $\gamma_0$. Then $\phi'(\xi_1) > 0$ and $\phi''(\xi_1) = 0$. From the definition of $\xi_1$ we obtain that $\phi'''(\xi_1) \le 0$ (since $\phi'' > 0$ in a left neighbourhood of $\xi_1$). From the definition of $\gamma_0$ we infer that $\phi'''(\xi_1) = 0$ since otherwise, by the implicit function theorem, $\xi_1 < \xi_2$ for $\gamma \in (\gamma_0 - \delta, \gamma_0)$ for some small positive $\delta$, contradicting the definition of $\gamma_0$.

It follows from Equation (3) that

$$\sin\phi - \gamma = \phi''' - \alpha\phi' < 0, \qquad \text{at } \xi_1, \tag{11}$$

hence $\phi(\xi_1) \in (\phi_1, \frac{3\pi}{2}) \subset (\frac{\pi}{2}, \frac{3\pi}{2})$; recall that $\phi_1$ is the second equilibrium. Differentiating (3) we obtain

$$\phi'''' = \alpha\phi'' + \phi'\cos\phi < 0, \qquad \text{at } \xi_1. \tag{12}$$

The fact that $\phi''''(\xi_1) < 0$ implies that $\phi'' < 0$ in a left neighbourhood of $\xi_1$, contradicting the definition of $\xi_1$. □

We now turn to the proof of Lemma 3.

**Proof of Lemma 3:**
**Part a.** For $\gamma=-1$ it follows immediately from the $z$-equation (6) that $\ddot{z}(t)\geq 0$ for all $t>\phi_0$, hence $\phi''(\xi)>0$ for all $\xi\in\mathbb{R}$.

**Part b.** Suppose, by contradiction, that $\gamma_0\leq 0$. Observe that $\phi_1\geq\pi$, and from Lemma 4 we see that $\dot{z}(t)>0$ on $(\phi_0,\frac{3\pi}{2})$. Since $\dot{z}(\frac{3\pi}{2})=0$ we have

$$0=\int_{\phi_0}^{\frac{3\pi}{2}}\ddot{z}(t)dt=\int_{\substack{t\in[\phi_0,\frac{3\pi}{2}]\\ \ddot{z}>0}}\ddot{z}(t)dt-\int_{\substack{t\in[\phi_0,\frac{3\pi}{2}]\\ \ddot{z}<0}}|\ddot{z}(t)|dt. \tag{13}$$

On the one hand we conclude from the above observations that (we use the notation $(y)_+\stackrel{\text{def}}{=}\max\{0,y\}$)

$$\begin{aligned}\int_{\substack{t\in[\phi_0,\frac{3\pi}{2}]\\ \ddot{z}<0}}|\ddot{z}(t)|\,dt&\leq\int_{\pi}^{\frac{3\pi}{2}}\Big(-\alpha-\frac{\sin t-\gamma_0}{\sqrt{2z(t)}}\Big)_+\,dt\leq\int_{\pi}^{\frac{3\pi}{2}}-\frac{\sin t}{\sqrt{2z(t)}}\,dt\\&<\int_{\pi}^{\frac{3\pi}{2}}-\frac{\sin t}{\sqrt{2z(\pi)}}\,dt=\frac{1}{\sqrt{2z(\pi)}},\end{aligned}\tag{14}$$

while on the other hand

$$\begin{aligned}\int_{\substack{t\in[\phi_0,\frac{3\pi}{2}]\\ \ddot{z}>0}}\ddot{z}(t)\,dt&\geq\int_{\frac{\pi}{2}}^{\pi}\alpha+\frac{\sin t-\gamma_0}{\sqrt{2z(t)}}\,dt\geq\int_{\frac{\pi}{2}}^{\pi}\frac{\sin t}{\sqrt{2z(t)}}\,dt\\&>\int_{\frac{\pi}{2}}^{\pi}\frac{\sin t}{\sqrt{2z(\pi)}}\,dt=\frac{1}{\sqrt{2z(\pi)}}.\end{aligned}\tag{15}$$

These inequalities contradict Equation (13).

**Part c.** Suppose, by contradiction, that $\gamma_0=1$. Then

$$\dot{z}(t)\geq 0\qquad\text{for } t\in[\frac{\pi}{2},\frac{3\pi}{2}]. \tag{16}$$

Also, $\ddot{z}(t)=\alpha+\frac{\sin t-1}{\sqrt{2z}}\leq\alpha$ for $t\in(\frac{\pi}{2},\frac{3\pi}{2}]$, from which we conclude that

$$z(t)\leq\frac{\alpha}{2}(t-\tfrac{\pi}{2})^2. \tag{17}$$

Now we find that

$$\dot{z}(\tfrac{3\pi}{2})=\int_{\frac{\pi}{2}}^{\frac{3\pi}{2}}\ddot{z}(t)\,dt\leq\int_{\frac{\pi}{2}}^{\frac{3\pi}{2}}\alpha+\frac{\sin t-1}{\sqrt{\alpha}(t-\frac{\pi}{2})}\,dt=\alpha\pi-\frac{C}{\sqrt{\alpha}}, \tag{18}$$

where

$$C\stackrel{\text{def}}{=}\int_{\frac{\pi}{2}}^{\frac{3\pi}{2}}\frac{\sin t-1}{(t-\frac{\pi}{2})}\,dt=\int_0^{\pi}\frac{1-\cos s}{s}\,ds. \tag{19}$$

Hence

$$\dot{z}(\tfrac{3\pi}{2}) < 0 \qquad \text{if} \quad \alpha\pi - \frac{C}{\sqrt{\alpha}} < 0, \text{ i.e. if } \alpha \leq \alpha_0 \stackrel{\text{def}}{=} \left(\frac{C}{\pi}\right)^{1/3}, \tag{20}$$

contradicting (16). Notice that $\alpha_0 \stackrel{\text{def}}{=} (\frac{C}{\pi})^{1/3} \gtrapprox 0.65$. □

# 3 Assumptions

Now we will highlight the other necessary conditions for the existence of the aforementioned spiral.

**5 Definition** *In this work with a spiral is meant a curve, converging to a point $x_0$, which can be parameterised in polar coordinates around $x_0$ as $r(\theta)$, where $r$ has the property that for all $\theta$, it holds that $r(\theta + 2\pi) < r(\theta)$. (Or for which it holds that for all $\theta$, $r(\theta + 2\pi) > r(\theta)$.)*

In the general setting we study a system

$$\dot{x} = f(x;p) \qquad x \in \mathbb{R}^3; p \in \mathbb{R}^2; f \in C^k \tag{21}$$

containing two hyperbolic equilibria $x_1$ and $x_2$. We will assume the equilibria to be independent of $p$, to simplify notation.

We assume

H1
$$\begin{aligned} \dim W^u(x_1;p) &= 1 \\ \dim W^s(x_1;p) &= 2 \\ \dim W^u(x_2;p) &= 2 \\ \dim W^s(x_2;p) &= 1 \end{aligned}$$

More specifically we assume

H2 The unstable eigenvalues of $x_2$ form a complex conjugate pair

Furthermore we assume that there exists a heteroclinic cycle $\Gamma_0 \cup \Gamma_1$ for $p = 0$:

H3
$$W^u(x_1;0) \cap W^s(x_2;0) = \Gamma^0,$$

and

H4
$$W^u(x_2;0) \cap W^s(x_1;0) \supset \Gamma^1,$$

(see Figure 3).

It is also assumed that $W^u(x_2;0)$ and $W^s(x_1;0)$ intersect transversally,

H5
$$T_qW^u(x_2;0) + T_qW^s(x_1;0) = \mathbb{R}^3, \quad q \in \Gamma^1.$$

Hence we have

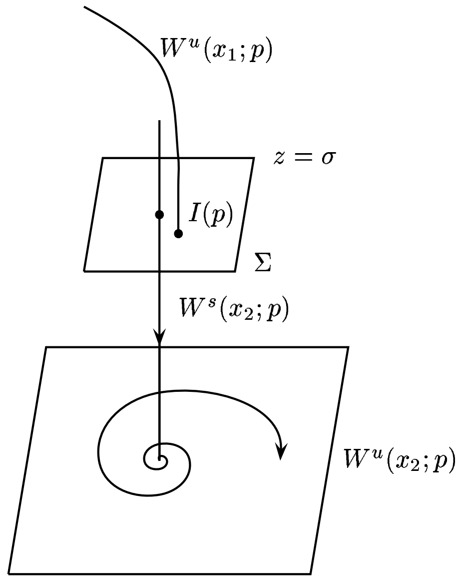


Figure 4: The flow near $x_2$

**6 Corollary** *For $p$ small enough there exists a one dimensional intersection of $W^u(x_2;p)$ and $W^s(x_1;p)$, this intersection will be denoted by $\Gamma^1(p)$.*

The intersection of $W^u(x_1;0)$ and $W^s(x_2;0)$ will in general not persist under perturbations. For small changes in the parameter $p$, $W^u(x_1;p)$ will still come close to the equilibrium $x_2$. We select a coordinate system around $x_2$, such that locally the stable manifold of $x_2$ is the $z$-axis and the unstable manifold is the $(x,y)$-plane $(\forall |p| < \delta_2)$. We take a transverse intersection of the stable manifold

$$\Sigma = \{(x,y,z) | z = \sigma\}$$

At $p=0$, the unstable manifold of $x_1$ will intersect $\Sigma$ at $(0,0,\sigma)$ (see Figure 4). We choose $\delta_2$ small enough such that for $|p| < \delta_2$ the unstable manifold of $x_1$ intersects $\Sigma$ for the first time at the point $I(p) = (x_I(p), y_I(p), \sigma)$.

Let $C_p$ be the set of parameter values for which there exist an orbit homoclinic to $x_1$ and let $I(p)$ be the first intersection of $W^u(x_1;p)$ with $\Sigma$. If $C_\Sigma$ denotes the intersection of the homoclinic orbits with $\Sigma$, then the relation between $C_\Sigma$ and $C_p$ is given by $C_p = I^{-1}(C_\Sigma)$. We assume $p \mapsto I(p)$ to be a bijection:

H6 $$\det \begin{bmatrix} \frac{\partial x_I}{\partial p_1} & \frac{\partial y_I}{\partial p_1} \\ \frac{\partial x_I}{\partial p_2} & \frac{\partial y_I}{\partial p_2} \end{bmatrix} \Bigg|_{p=0} \neq 0.$$

We want hypothesis H6 to be satisfied for all small $\sigma > 0$. This can be reformulated in a more convenient way by using the solutions to the variation equations, where we consider variations around the special heteroclinic orbit $\Gamma_0$. We call $\phi_{p_1}$ the solution of the variation equation of (21) around $\Gamma_0$ for variations in $p_1$, and in the same way define $\phi_{p_2}$. The solution of the variation equation for variations in time will be denoted by $\phi_t$. Assumption H6 can now be reformulated as assuming that the solutions $\phi_{p_1}$, $\phi_{p_2}$ and $\phi_t$ are linearly independent, close to the right hand equilibrium:

H6b $$\lim_{\xi\to\infty} \det \underbrace{\begin{bmatrix}\phi_{p_1} & \phi_{p_2} & \phi_t\end{bmatrix}}_{B} \neq 0$$

If H6b is satisfied then it follows that H6 holds for all sufficiently small $\sigma$.

# 4 Local Analysis

We will first formulate the desired result in a theorem.

**7 Theorem** *Under the assumptions H1–H5&H6b, there exists $\delta_2 > 0$ and a curve in parameter space $(p_1(\eta), p_2(\eta))$, defined for $|\eta| < \delta_2$ for which there exists an orbit homoclinic to $x_1$. Furthermore this curve will be a spiral.*

**Proof:**
It is convenient to use cylindrical coordinates. We choose a $\rho > 0$ small enough and a $C^1$-coordinate transformation such that for $r \leq \rho$ and $z \leq \sigma$, the system is locally given by

$$\begin{cases} \dot{r} = \mu, \\ \dot{\theta} = \omega, \\ \dot{z} = -\lambda. \end{cases} \tag{22}$$

In the present case $C^1$-linearisation is possible, see [6].

According to Lemma 6 there exists, for $|p|$ small enough, a connection $\Gamma^1(p)$, which intersects the cylinder $r = \rho$ at the position $Q = (\rho, \theta_0(p), 0)$. Since the intersection of $W^u(x_2;p)$ and $W^s(x_1;p)$ is transversal, there exists a function $\theta^s(z;p)$, such that the stable manifold of $x_1$ contains the curve $C_1(z) = (\rho, \theta^s(z;p), z)$ for $|z|$ small enough (see Figure 5), and $\theta^s(z;p)$ is $C^1$ for small $z$ and $p$.

We will now show that for certain values of $p$ the unstable manifold of $x_1$, intersecting $\Sigma$ at $I(p) = (r_I(p), \theta_I(p), \sigma)$, (with $r_I < \rho$) will intersect this curve $C_1(z)$.

Because of H6 we can locally write $p(r_I, \theta_I)$.

The curve through $I(p(r_I, \theta_I))$ is for $t \geq 0$ parameterised by

$$\begin{cases} r = r_I e^{\mu t}, \\ \theta = \theta_I + \omega t, \\ z = \sigma e^{-\lambda t}. \end{cases} \tag{23}$$

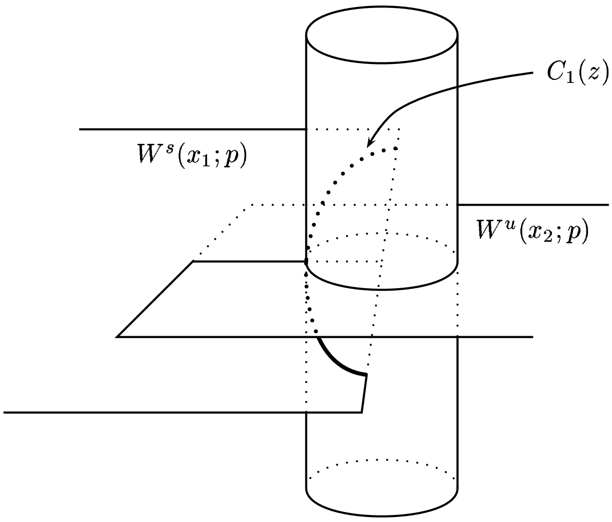


Figure 5: The curve $C_1$ is the intersection of $W^s(x_1;p)$ with a cylinder.

This curve will intersect the cylinder $r = \rho$ at a time

$$t = \frac{\ln \frac{\rho}{r_I}}{\mu} \tag{24}$$

so the intersection point will be $(\rho, \theta_I + \frac{\omega}{\mu} \ln \frac{\rho}{r_I}, \sigma \left(\frac{\rho}{r_I}\right)^{-\frac{\lambda}{\mu}})$.

Thus this curve will intersect the stable manifold of $x_1$ if it intersects the curve $C_1$, i.e.

$$\theta^s(\sigma \left(\frac{\rho}{r_I}\right)^{-\frac{\lambda}{\mu}}; p(r_I, \theta_I)) = \theta_I + \frac{\omega}{\mu} \ln \frac{\rho}{r_I} \mod 2\pi. \tag{25}$$

The left-hand side of this equation approaches a constant, say $\theta_0 = \theta^s(0;0)$, as $r_I \to 0$. Hence it is easily seen that the $(r_I, \theta_I)$ satisfying (25) form a spiral for small $r_I$, since we find that, with $\kappa = \min\{1, \frac{\lambda}{\mu}\} > 0$,

$$\theta_I = -\frac{\omega}{\mu} \ln \frac{\rho}{r_I} + \theta_0 + \mathcal{O}(r_I^\kappa) \qquad \text{as } r_I \to 0. \tag{26}$$

□

# 5 Verification of the assumptions

As mentioned in the Introduction, the motivation for this analysis was the observed phenomenon in the equation

$$\beta c\phi''' + (1-c^2)\phi'' - \alpha c\phi' - \sin\phi + \gamma = 0, \tag{27}$$

which we write in the form

$$\begin{aligned} \phi' &= \psi \\ \psi' &= \chi \\ \chi' &= \frac{-(1-c^2)}{\beta c}\chi + \frac{\alpha}{\beta}\psi + \frac{\sin\phi - \gamma}{\beta c} \end{aligned} \tag{28}$$

We will verify that the assumptions H1–H6b hold. As mentioned in the Introduction, $\phi$ is an angle-variable, hence the equilibria $\phi_{2k}$ will be identified and denoted by $x_2$, and $\phi_{2k+1}$ will be denoted by $x_1$.

The assumptions about the dimensions are satisfied. It is also easily checked that H2 is satisfied. The existence of a heteroclinic solution has been proven in section 2. The following subsections will be dedicated to checking the conditions H4–H6b numerically. For this we will make use of the program AUTO [4].

The values of the parameters have been chosen to be the same as those in [2], this means $\alpha = 0.18$, $\beta = 0.1$. We obtained a slightly different value for $\gamma^*$, namely $\gamma^* = 0.8830437$. We note that $\tilde{\alpha} = \frac{\alpha}{\sqrt[3]{\beta}} \approx 0.39$ is within the range covered by Theorem 2.

## 5.1 Bijection

The condition H6b was checked by calculating the determinant of the matrix $B$ defined in H6b. However, we did not directly use the solutions to the variation equations. Near the equilibrium $x_2$, both $\phi_c$ and $\phi_\gamma$ might increase exponentially, while $\phi_t$ will decrease exponentially (the determinant, however, will remain finite). We defined $\hat{\phi}_t = \frac{\phi_t}{|\phi_t|}$, which is the direction of $\phi_t$ and which must satisfy

$$\frac{d}{d\xi}\hat{\phi} = A(\xi)\hat{\phi} - \hat{\phi} < A(\xi)\hat{\phi}, \hat{\phi} >, \tag{29}$$

where $A(\xi) = Df(\Gamma^0(\xi))$ and the vector $f$ represents the right hand side of (28). For $\phi_c$ and $\phi_\gamma$ we know the growth behaviour near $x_2$ and define $\hat{\phi}_c = e^{-\lambda\xi}\phi_c$, where $\lambda$ is the real part of the complex eigenvalues of $x_2$, and we solve the equation for $\hat{\phi}_c$ instead of $\phi_c$ (and similarly for $\phi_\gamma$).

In Figure 6 the determinant is plotted as a function of $\xi$ (rescaled to lie in the interval [0,1]). The determinant is very small, since the three vectors are almost co-planar. However, as can be seen, the determinant does not vanish

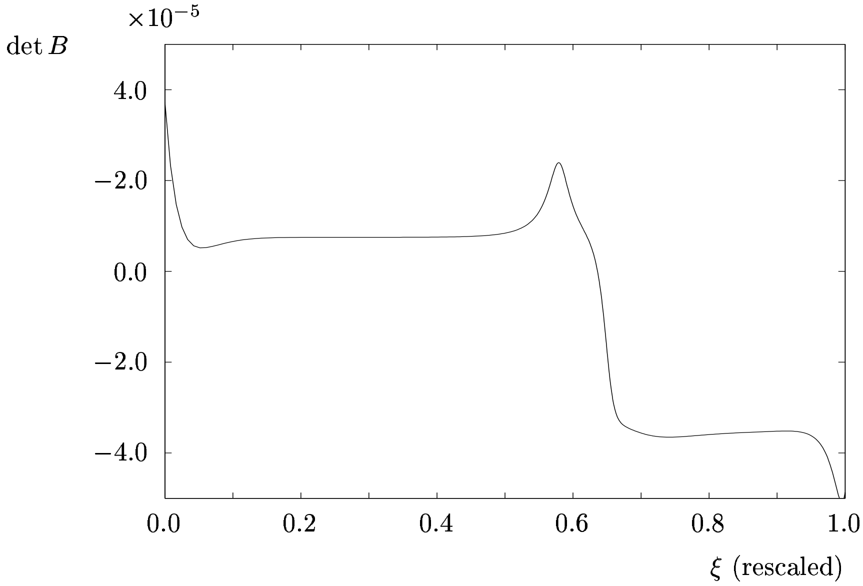


Figure 6: The determinant as a function of $\xi$.

near the right hand equilibrium ($\xi \approx 1.0$). Near the right hand equilibrium, the determinant should be constant. In the figure it does not stay constant all the way, but this is caused by numerical errors (numerically the approach to the equilibrium is not *exactly* along the stable eigenvector).

## 5.2 Transversality

Now we will indicate how the assumptions H4 and H5 were checked.

To calculate the intersection of the two manifolds, the calculation was set up as follows. First, using DSTOOL [5], we found a starting point, close to $x_2$, which lies on a trajectory that passes close to the left hand equilibrium $x_1$. A solution starting from this point was then used as an initial condition to a boundary value problem for AUTO. The solution was required to start in the unstable eigenspace of the equilibrium $x_2$ and was calculated, until it hit the stable eigenspace of the equilibrium $x_1$. In a further step the distance to both equilibria was decreased, hence the solution converged to the heteroclinic solution.

To check the transversality condition, we calculated the linear approximation to both manifolds and the angle $\theta_M$ between them. The linear approximation to one of these manifolds is spanned by the direction of the intersection and a solution to the variation equation.

Also in this case we did not directly calculate solutions to the variation equation, since we are only interested in the direction of the solution and these solutions will diverge rapidly. If the intersection is given by $q(\xi)$, the variation equation is given by

$$\dot{y} = Df(q(\xi))y. \tag{30}$$

We did not solve for $y$, but defined $v = \frac{y}{|y|}$, similar to what we did to check condition H6b. We calculated two solutions $v_l$ and $v_r$ to the variation equation, where $v_l(0)$ was required to be perpendicular to the intersection and to lie in the stable eigenspace of $x_1$, whereas $v_r(1)$ was required to lie in the unstable eigenspace of $x_2$ (time is rescaled so that $\xi = 1$ is the end-point). For every point $\xi$, the linear approximation to the unstable manifold of $x_2$ is thus spanned by $\dot{q}(\xi)$ and $v_l(\xi)$. Hence we could calculate the angle $\theta_M$ made by the two manifolds at any point and hence check the transversality condition. The angle between the manifolds was always larger than 0.5 rad.

### 5.3 Conclusions

For the model of a long Josephson junction the spiral in the $(c, \gamma)$-plane, the points on which are parameter combinations for which a homoclinic solution exists, is explained. To do this we proved the existence of a heteroclinic orbit, making use of the fact that this heteroclinic orbit is monotone and that the system is reversible at that particular value of the parameters. That there is a spiral in parameter space then follows from a local analysis similar to the one of Bykov [3]. The hypotheses we needed to assume for the proof were checked numerically for specific values (taken from [2]) of the parameters.

## References


[1] A Barone and G Paterno. *Physics and Applications of the Josephson Effect.* John WIley & Sons, 1982.

[2] D.L. Brown, M.G. Forest, et al. Computation and stability of fluxons in a singularly perturbed sine-gordon model of the long josephson junction. *SIAM Journal on Applied Mathematics*, 54(4):1048–1066, 1994.

[3] V.V. Bykov. Orbit structure in a neighborhood of a separatrix cycle containing two saddle-foci. *Americal Mathematical Society Translates 2*, 200:87–97, 2000.

[4] E.J. Doedel, A.R. Champneys, et al. *AUTO 97: Continuation and bifurcation software for ordinary differential equation (with HomCont).* Concordia University, Canada, `ftp.ca.concordia.ca/pub/doedel/auto`.

[5] J. Guckenheimer, M.R. Myers, et al. *DsTool: A Dynamical System Toolkit with an Interactive Graphical Interface.* Cornell University, `http://www.geom.umn.edu/software/dstool/`.

[6] S. Sternberg. Local contractions and a theorem of poincaré. *American Journal of Mathematics*, 79:809–824, 1957.

[7] J.F. Toland. Existence and uniqueness of heteroclinic orbits for the equation $\lambda u''' + u' = f(u)$. *Proceedings of the Royal Society of Edinburgh*, 109A:23–26, 1988.